JOURNAL OF PROPULSION AND POWER
Vol. 11, No. 1, January–February 1995

# Numerical Analysis of Rarefied Gas Flow Through Two-Dimensional Nozzles

Chan-Hong Chung*
*NASA Lewis Research Center, Cleveland, Ohio 44133*
and
Kenneth J. De Witt,† Duen-Ren Jeng,‡ and Theo G. Keith Jr.§
*University of Toledo, Toledo, Ohio 43606*

**A kinetic-theory analysis is made of the flow of a rarefied gas from one reservoir to another through two-dimensional nozzles with arbitrary contour. The Boltzmann equation, simplified by the Bhatnagar, Gross, and Krook model for the collision integral, is solved by means of finite difference approximations with the discrete ordinate method. The physical space is transformed by a general grid-generation technique, and the velocity space is transformed to a polar coordinate system. A numerical code is developed that can be applied to any two-dimensional passage of complicated geometry for the flow regimes from free-molecular to slip. Numerical values of flow quantities can be calculated for the entire physical space, including both inside the nozzle and in the outside plume. Predictions are made for the case of parallel slots and compared with existing literature data. Also, results for the cases of convergent or divergent slots and two-dimensional nozzles with arbitrary contour at arbitrary Knudsen number are presented.**

## Introduction

THE flow of a rarefied gas through channels is one of the important problems in the field of gas dynamics. Applications of this type of flow are in vacuum science, molecular beam technology, and high-altitude flight such as the flowfield for low-thrust resistojets. Many investigations have been reported for simple geometries such as a slit,[1,2] an orifice,[1,3] a two-dimensional slot,[4–8] and a circular tube.[9,10]

Wang and Yu[4] studied nearly free-molecular flow through a two-dimensional slot by integrating the Boltzmann equation with the Bhatnagar, Gross, and Krook (BGK) model[11] along a characteristic. They decomposed the distribution function into three parts and obtained a first-order correction to the flux at a free-molecular flow condition. Raghuraman and Willis[5] solved the Boltzmann equation with the BGK model by the moment and discrete ordinate methods and obtained a mass flux and a wall number flux. Unfortunately, their results show step-like variations in the wall flux, which is incorrect in a physical sense. Yamamoto and Asai[6] used the same method as that of Wang and Yu, and developed a more rigorous analysis. Fujimoto and Usami[7] studied an infinite pressure ratio case using the direct simulation Monte Carlo (DSMC) method developed by Bird[12] and compared their results with experimental data. Usami et al.[8] investigated a mass flow reduction due to the roughness of a slot surface using the DSMC method.

Theoretical analysis of the flowfield through more complex geometries than a parallel slot or a circular tube is rather difficult to treat, and few studies have been done in this area. Reynolds and Richley[9] studied the free-molecular flowfield through convergent or divergent slots, and conical tubes by solving a Clausing-type integral equation. Füstöss[10] used the DSMC method to study near free-molecular flow through conical tubes. Recently, Riley and Scheller[13] studied a flowfield around a divergent nozzle by integrating the Boltzmann equation with the BGK model along a characteristic. However, in calculating the flowfield inside the nozzle, they approximated the number density at the nozzle wall using the density and temperature at the centerline and neglected slip at the nozzle wall.

In the current study, a kinetic-theory analysis has been made of the flow of a rarefied gas from one reservoir to another through two-dimensional nozzles with arbitrary contour to study the effect of nozzle design on the induced molecular flow environment. The flow regimes cover the range from free-molecular to slip flow. Flows through simpler geometries such as a slit, parallel slot, and convergent or divergent slots are included as special cases.

The Boltzmann equation simplified by a collision model is solved by means of a finite-difference approximation. The physical space is transformed by a general grid-generation technique, and both simple explicit and implicit algorithms are used depending on the characteristics of the velocity space. The velocity space is transformed to a polar coordinate and the concept of the discrete ordinate method is employed to discretize the velocity space. The modified Gauss-Hermite quadrature[14,15] and Simpson's rule are used for the discretized velocity space.

A computer code is developed that can essentially be applied to any two-dimensional passage of complicated geometry for the flow regimes from free-molecular to slip. In this code, numerical values of flow quantities such as density, velocity, temperature, and shear stress can be calculated for the entire physical space, including both inside the nozzle and in the outside plume.

Calculations are made for the cases of parallel, convergent, and divergent slots at an arbitrary Knudsen number and compared with existing literature data. Also, the flowfield around a convergent-divergent nozzle with a curved surface is calculated at arbitrary Knudsen number.

## Formulation of the Problem

### Governing Equation

We consider the steady-state Boltzmann equation without an external force in a Cartesian coordinate system, as illus-

Received Nov. 1, 1990; revision received July 22, 1993; accepted for publication Dec. 15, 1993. 

*Resident Research Associate, Computational Methods for Space Branch. Member AIAA.

†Professor, Chemical Engineering Department. Member AIAA.

‡Professor, Mechanical Engineering Department. Member AIAA.

§Professor, Mechanical Engineering Department. Associate Fellow AIAA.

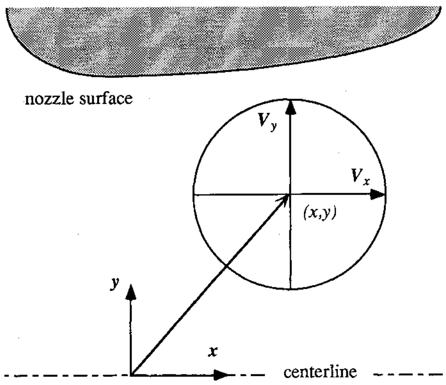


**Fig. 1 Coordinate system.**

trated in Fig. 1

$$V_x \frac{\partial f}{\partial x} + V_y \frac{\partial f}{\partial y} = J \tag{1}$$

where $x$ and $y$ are Cartesian coordinates of the physical space, $V_x$ and $V_y$ are the velocity components of the molecules, $f(x, y, V_x, V_y, V_z)$ is the distribution function, and $J$ is the collision integral, which is some functional of $f$. The moments $n$, $\boldsymbol{U}$, $T$, and $\boldsymbol{\tau}$ are given by

$$n = \int f \, \mathrm{d}\boldsymbol{V} \tag{2a}$$

$$n\boldsymbol{U} = \int \boldsymbol{V} f \, \mathrm{d}\boldsymbol{V} \tag{2b}$$

$$3nRT = \int C^2 f \, \mathrm{d}\boldsymbol{V} \tag{2c}$$

$$\boldsymbol{\tau} = -m \int \boldsymbol{C}\boldsymbol{C} f \, \mathrm{d}\boldsymbol{V} \tag{2d}$$

where $R$ denotes the gas constant, $n$ the particle density, $\boldsymbol{U}$ the macroscopic flow velocity, $T$ the temperature, $\boldsymbol{\tau}$ the viscous stress, $m$ the mass of a single molecule, and $\boldsymbol{C}$ the peculiar velocity, defined as $\boldsymbol{V} - \boldsymbol{U}$.

#### Collision Integral

A solution of the Boltzmann equation is an exceedingly formidable task due to the complicated structure of the collision integral, which contains the details of the molecular interaction. In order to avoid the complex Boltzmann collision integral, several kinetic model equations for monatomic gases such as BGK,[11] Ellipsoidal,[16] and S model,[17,18] etc., have been proposed. These models retain the fundamental features of molecular collision and average properties of the Boltzmann integral, and have been extended to gases with internal degrees of freedom (DOF)[19,20] and to multicomponent gases.[21–23] The collision integral of the kinetic models $J_m$, can be represented generally in a form

$$J_m = A_c(F - f) \tag{3}$$

Here, $A_c F$ approximates the replenishing collisions, and $A_c f$ the depletion collisions. The collision frequency $A_c$ usually is a function of moments and is independent of molecular velocities, whereas $F$ is a function of both moments and molecular velocities.

#### Reduced Distribution Function

To reduce the number of independent variables, the following reduced distribution functions are introduced:

$$g(x, y, V_x, V_y) = \int_{-\infty}^{+\infty} f(x, y, V_x, V_y, V_z) \, \mathrm{d}V_z \tag{4a}$$

$$h(x, y, V_x, V_y) = \int_{-\infty}^{+\infty} V_z^2 f(x, y, V_x, V_y, V_z) \, \mathrm{d}V_z \tag{4b}$$

These kinds of functions were first applied by Chu[24] in analyzing the unsteady plane shock problem, and afterward by many investigators.[25,26] The corresponding equations for the reduced distribution functions with the collision integral of kinetic models of Eq. (3) are obtained from Eq. (1) by integrating out the $V_z$ dependence with the weighting functions 1 and $V_z^2$, respectively:

$$V_z \frac{\partial g}{\partial x} + V_y \frac{\partial g}{\partial y} + A_c g = A_c G \tag{5a}$$

$$V_x \frac{\partial h}{\partial x} + V_y \frac{\partial h}{\partial y} + A_c h = A_c H \tag{5b}$$

where

$$G(x, y, V_x, V_y) = \int_{-\infty}^{+\infty} F \, \mathrm{d}V_z$$

$$H(x, y, V_x, V_y) = \int_{-\infty}^{+\infty} V_z^2 F \, \mathrm{d}V_z$$

#### Nondimensionalization

Using the characteristic length of a flowfield $d$, and the most probable speed $V_0$, defined as

$$V_0 = (2RT_0)^{1/2} \tag{6}$$

the following dimensionless variables are introduced:

$$\hat{x} = x/d, \quad \hat{y} = y/d, \quad \hat{n} = n/n_0$$

$$\hat{V}_i = V_i/V_0, \quad \hat{U}_i = U_i/V_0, \quad \hat{T} = T/T_0$$

$$\hat{\tau} = \tau/(mn_0V_0^2), \quad \hat{A}_c = A_c d/V_0, \quad \hat{g} = gV_0^2/n_0$$

$$\hat{h} = h/n_0, \quad \hat{G} = GV_0^2/n_0, \quad \hat{H} = H/n_0$$

where the subscript 0 refers to an upstream reservoir condition.

#### Transformation of Velocity Space

For the Cartesian velocity space $(\hat{V}_x, \hat{V}_y)$, we introduce a polar coordinate system, which is defined as

$$\hat{V}_x = V \sin\phi, \quad \hat{V}_y = V\cos\phi, \quad \text{and} \quad \phi = \tan^{-1}(\hat{V}_x/\hat{V}_y) \tag{7}$$

With this polar coordinate system, Eq. (5) can be written as

$$V \sin\phi \frac{\partial \hat{g}}{\partial \hat{x}} + V\cos\phi \frac{\partial \hat{g}}{\partial \hat{y}} + \hat{A}_c \hat{g} = \hat{A}_c \hat{G} \tag{8a}$$

$$V \sin\phi \frac{\partial \hat{h}}{\partial \hat{x}} + V\cos\phi \frac{\partial \hat{h}}{\partial \hat{y}} + \hat{A}_c \hat{h} = \hat{A}_c \hat{H} \tag{8b}$$

#### Transformation of Physical Space

In the development of a numerical procedure for solving the governing equations, the first step is to superimpose a grid distribution over the flow domain. For irregularly shaped flow domains, numerical methods of generating the grid have been widely used over the past several years. Grid-generation techniques have gained importance in the numerical solution of partial differential equations. Recent developments provide a variety of methods to generate and control the grid for better quality solutions. A comprehensive review of this subject can be found elsewhere.[27,28]

In the current study, the method developed by Thomas and Middlecoff[29] is adopted for the flow domain inside a nozzle.

Outside the nozzle, the following transformations are used for the $y$ coordinate:

$$\eta = [1 - \exp(t_n\hat{y}/D)]/[1 - \exp(t_n)] \quad \text{for} \quad 0 \le \hat{y} \le D \tag{9a}$$

$$\eta = 2 - \exp[t_y(1 - \hat{y}/D)] \quad \text{for} \quad D \le \hat{y} \le \infty \tag{9b}$$

where $D$ is chosen to be $Y_0/d$ at the upstream reservoir, and $Y_d/d$ at the downstream reservoir. The quantities $Y_0$ and $Y_d$ are the inlet and exit half-widths of the nozzle, respectively. For the $x$ coordinate, the transformations

$$\xi = 2 - \exp[t_x(1 - \hat{x}/D)] \tag{10a}$$

$$\xi = -2 + \exp[t_x(1 + \hat{x}/D)] \tag{10b}$$

are used for the upstream and downstream reservoirs, respectively. The quantity $D$ is chosen to be $L/2d$, where $L$ is the length of the nozzle. Here, $t_n$, $t_y$, and $t_x$ are stretching parameters.

Once the curvilinear coordinates are generated for a given flow domain, the governing equations must be transformed in terms of these coordinates. According to general transformation rules, the governing equations in the new coordinate system are written as

$$B\frac{\partial \hat{g}}{\partial \eta} + C\frac{\partial \hat{g}}{\partial \xi} + \hat{A}_c\hat{g} = \hat{A}_c\hat{G} \tag{11a}$$

$$B\frac{\partial \hat{h}}{\partial \eta} + C\frac{\partial \hat{h}}{\partial \xi} + \hat{A}_c\hat{h} = \hat{A}_c\hat{H} \tag{11b}$$

where

$$B = (V\cos\phi\hat{x}_\xi - V\sin\phi\hat{y}_\xi)/J_t$$

$$C = (V\sin\phi\hat{y}_\eta - V\cos\phi\hat{x}_\eta)/J_t$$

Here, $J_t$ denotes the Jacobian of the transformation.

## Computational Procedure

### Discrete Ordinate Method

In order to remove the velocity space dependency from the reduced distribution functions, the discrete ordinate method[25] is employed. This method, which consists of replacing the integration over velocity space of the distribution functions by appropriate integration formulas, requires the values of the distribution functions only at certain discrete speeds and velocity angles. The choice of the discrete values of $V$ and $\phi$ are dictated by the consideration that our final interest is not in the distribution functions themselves, but in the moments. Hence, the macroscopic moments given by integrals over the molecular velocity space can be calculated by proper integration formulas. Applying the method, the following quadratures are substituted for the integrals in Eq. (2):

$$\hat{n} = \sum_\delta \int_0^{2\pi} P_\delta \hat{g}_\delta \, d\phi \tag{12a}$$

$$\hat{n}\hat{U}_x = \sum_\delta \int_0^{2\pi} P_\delta V_\delta \sin\phi \hat{g}_\delta \, d\phi \tag{12b}$$

$$\hat{n}\hat{U}_y = \sum_\delta \int_0^{2\pi} P_\delta V_\delta \cos\phi \hat{g}_\delta \, d\phi \tag{12c}$$

$$\frac{3}{2}\hat{n}\hat{T} = \sum_\delta \int_0^{2\pi} P_\delta(\hat{h}_\delta + V_\delta^2\hat{g}_\delta)\, d\phi - \hat{n}(\hat{U}_x^2 + \hat{U}_y^2) \tag{12d}$$

$$\hat{\tau}_{xy} = -\sum_\delta \int_0^{2\pi} P_\delta V_\delta^2 \sin\phi\cos\phi\, \hat{g}_\delta \, d\phi + \hat{n}\hat{U}_x\hat{U}_y$$

$$(\delta = 1, 2, 3, \ldots, N-1, N) \tag{12e}$$

where $P_\delta$ is the weighting factor of the quadrature for the discrete speed $V_\delta$, and $\hat{g}_\delta$ and $\hat{h}_\delta$ denote $\hat{g}(\xi, \eta, V_\delta, \phi)$ and $\hat{h}(\xi, \eta, V_\delta, \phi)$, respectively. Thus, instead of solving the equations for a function of space and molecular velocity, the equations are transformed to partial differential equations that are continuous in space, but are point functions in molecular speed $V$ and velocity angle $\phi$, as follows:

$$B\frac{\partial \hat{g}_\delta}{\partial \eta} + C\frac{\partial \hat{g}_\delta}{\partial \xi} + \hat{A}_c\hat{g}_\delta = \hat{A}_c\hat{G}_\delta \tag{13a}$$

$$B\frac{\partial \hat{h}_\delta}{\partial \eta} + C\frac{\partial \hat{h}_\delta}{\partial \xi} + \hat{A}_c\hat{h}_\delta = \hat{A}_c\hat{H}_\delta \tag{13b}$$

where

$$B = (V_\delta\cos\phi\hat{x}_\xi - V_\delta\sin\phi\hat{y}_\xi)/J_t$$

$$C = (V_\delta\sin\phi\hat{y}_\eta - V_\delta\cos\phi\hat{x}_\eta)/J_t$$

$$\hat{G}_\delta = \frac{V_0^2}{n_0}\int_{-\infty}^{\infty} f(\xi, \eta, V_\delta, \phi, V_z)\, dV_z$$

$$\hat{H}_\delta = \frac{1}{n_0}\int_{-\infty}^{\infty} V_z^2 f(\xi, \eta, V_\delta, \phi, V_z)\, dV_z$$

### Finite Difference Algorithm

Equation (13) is solved by means of finite difference approximations in physical space. To reduce CPU time, a simple explicit scheme is used for $\xi$:

$$\frac{\partial \hat{g}_\delta}{\partial \xi} \cong \frac{\hat{g}_\delta(\xi, \eta) - \hat{g}_\delta(\xi - js\Delta\xi, \eta)}{js\Delta\xi} \tag{14}$$

The following finite difference schemes are used for $\eta$, depending on the characteristics of physical and velocity space:

$$\frac{\partial \hat{g}_\delta}{\partial \eta} \cong \frac{\hat{g}_\delta(\xi, \eta) - \hat{g}_\delta(\xi, \eta - is\Delta\eta)}{is\Delta\eta} \tag{15}$$

$$\frac{\partial \hat{g}_\delta}{\partial \eta} \cong \frac{\hat{g}_\delta(\xi, \eta + \Delta\eta) - \hat{g}_\delta(\xi, \eta - \Delta\eta)}{2\Delta\eta} \tag{16}$$

$$\frac{\partial \hat{g}_\delta}{\partial \eta} \cong \frac{\hat{g}_\delta(\xi - js\Delta\xi, \eta) - \hat{g}_\delta(\xi - js\Delta\xi, \eta - is\Delta\eta)}{is\Delta\eta} \tag{17}$$

where

$$is = \mathrm{sign}[(V_\delta\cos\phi\hat{x}_\xi - V_\delta\sin\phi\hat{y}_\xi)/J_t]$$

$$js = \mathrm{sign}[(V_\delta\sin\phi\hat{y}_\eta - V_\delta\cos\phi\hat{x}_\eta)/J_t]$$

In the region outside the nozzle, scheme (15) is used. Inside the nozzle, the velocity space is divided into three regions as illustrated in Table 1. These regions depend on the tangent to the surface at any constant $\xi$ line, where $\phi_t$ is a velocity angle that is parallel to the surface tangent at any constant $\xi$ line. In regions (i) and (ii), schemes (15) and (16) are used, respectively. In region (iii), scheme (16) is used except at the

**Table 1 Division of velocity space**

| Surface tangent | Positive | Negative |
|---|---|---|
| Region (i) | $\pi/2 \le \phi \le \pi$ | $\phi_t \le \phi \le \pi/2$ |
| | $-\pi/2 \le \phi \le \phi_t$ | $\phi_t + \pi \le \phi \le \pi$ |
| | $-\pi \le \phi \le \phi_t - \pi$ | $-\pi \le \phi \le -\pi/2$ |
| Region (ii) | $\phi_t < \phi < \pi/2$ | $-\pi/2 < \phi < \phi_t$ |
| Region (iii) | $\phi_t - \pi < \phi < -\pi/2$ | $\pi/2 < \phi < \phi_t + \pi$ |

surface and centerline where scheme (17) is used by considering the common behavior of hyperbolic equations, i.e., a limited domain of dependency and a characteristic direction.[30] The following finite difference approximations of Eqs. (13) are obtained:

Using schemes (14) and (15)

$$(B_0 + C_0 + D_0)\hat{g}_\delta(\xi, \eta) = D_0\hat{G}_\delta + B_0\hat{g}_\delta(\xi, \eta - is\Delta\eta) + C_0\hat{g}_\delta(\xi - js\Delta\xi, \eta) \tag{18}$$

Using schemes (14) and (16)

$$B_{II}\hat{g}_\delta(\xi, \eta + \Delta\eta) + (C_0 + D_0)\hat{g}_\delta(\xi, \eta) - B_{II}\hat{g}_\delta(\xi, \eta - \Delta\eta) = D_0\hat{G}_\delta + C_0\hat{g}_\delta(\xi - js\Delta\xi, \eta) \tag{19}$$

Using schemes (14) and (17)

$$(C_0 + D_0)\hat{g}_\delta(\xi, \eta) = D_0\hat{G}_\delta + (C_0 - B_0)\hat{g}_\delta(\xi - js\Delta\xi, \eta) + B_0\hat{g}_\delta(\xi - js\Delta\xi, \eta - is\Delta\eta) \tag{20}$$

where

$$B_0 = is(\cos\phi\hat{x}_\xi - \sin\phi\hat{y}_\xi)/(J_t\Delta\eta)$$

$$C_0 = js(\sin\phi\hat{y}_\eta - \cos\phi\hat{x}_\eta)/(J_t\Delta\xi)$$

$$D_0 = \hat{A}_c/V_\delta$$

$$B_{II} = (\cos\phi\hat{x}_\xi - \sin\phi\hat{y}_\xi)/(2J_t\Delta\eta)$$

Taking equivalent finite difference schemes for $\hat{h}_\delta$, the system of nonlinear algebraic Eqs. (18–20) is to be solved by the method of successive approximations. In the iterative procedure, only the values of $\hat{A}_c$, $\hat{G}_\delta$, and $\hat{H}_\delta$ have to be determined from moments of the previous iteration, and the values of distribution functions do not need to be stored. Convergency is assumed to have occurred when the differences of the moments of two successive iteration steps are kept within the bound of prescribed tolerance at every spatial grid point.

#### Stability Analysis

To ensure the convergence of the finite difference approximations, consistency and stability are checked according to the equivalence theorem of Lax.[31] In the limit $\Delta\xi \to 0$ and $\Delta\eta \to 0$, consistency can be easily verified by reducing Eqs. (18–20) to Eq. (13). Von Neumann analysis is made for the linearized form of the finite difference approximations. It is quite straightforward to get the following restrictions:

$$B_0 \geq 0, \quad C_0 \geq 0, \quad \text{and} \quad (B_0 - C_0) \leq 0 \tag{21}$$

By choosing appropriate marching directions following the motion of each molecule both in physical and velocity space, the first two conditions in Eq. (21) already have been satisfied, and the last condition yields[30] the following restriction on the choice of stepwidth at the centerline of a nozzle:

$$(\Delta\eta/\Delta\xi) \geq S'(\xi)(\hat{x}_\xi/\hat{y}_\eta) \tag{22}$$

The quantity $S'(\xi)$ is the tangent to the surface at any constant $\xi$ line.

It should be noted that while one grants the utility of studying linear systems as guidelines to nonlinear systems, the application of the Lax equivalence theorem to nonlinear equations has to be regarded as an approximation due to the possible nonuniqueness of solutions of nonlinear equations.[32]

## Method of Solution

#### Model Equation

For the collision integral, the BGK model is chosen for the sake of simplicity. In this model, $F$ is given by the Maxwell-Boltzmann distribution:

$$F = n(2\pi RT)^{-3/2}\exp(-C^2/2RT) \tag{23}$$

The collision frequency $A_c$ is taken to be of the form[33]

$$A_c = mnRT/\mu \tag{24}$$

where the viscosity $\mu$ is assumed to have a temperature dependency[33]

$$(\mu/\mu_0) = (T/T_0)^\sigma \tag{25}$$

where $\sigma$ is a constant for a given gas. The viscosity at the upstream reservoir condition $\mu_0$ is related to the upstream mean free path $\lambda_0$ by the relation

$$\lambda_0 = \tfrac{16}{5}[\mu_0/mn_0(2\pi RT_0)^{1/2}] \tag{26}$$

The characteristic length of the flowfield $d$ is chosen as the nozzle inlet half-width $Y_0$, and the Knudsen number $Kn$ is defined as the ratio of the upstream mean free path to the nozzle inlet width $W = 2Y_0$.

#### Boundary Conditions

The following boundary conditions are used for the calculation. Far infinity in the upstream reservoir, there is an equilibrium distribution with prescribed reservoir conditions $\hat{n}_0$ and $\hat{T}_0$:

$$\hat{g} = (\hat{n}_0/\pi\hat{T}_0)\exp(-V^2/\hat{T}_0) \tag{27a}$$

$$\hat{h} = \tfrac{1}{2}\hat{T}_0\hat{g} \tag{27b}$$

Similarly, in the downstream reservoir

$$\hat{g} = (b\hat{n}_0/\pi\hat{T}_b)\exp(-V^2/\hat{T}_b) \tag{28a}$$

$$\hat{h} = \tfrac{1}{2}\hat{T}_b\hat{g} \tag{28b}$$

where $b\hat{n}_0$ and $\hat{T}_b$ are the number density and temperature in the reservoir, and $b$ is the density ratio between the two reservoirs.

In order to specify the interaction of the molecules with the surface, diffuse reflection is assumed, i.e., molecules that strike the surface are subsequently emitted with a Maxwell distribution characterized by the surface temperature $\hat{T}_w$

$$\hat{g} = (\hat{n}_w/\pi\hat{T}_w)\exp(-V^2/\hat{T}_w), \quad \text{for} \quad (V\cdot\boldsymbol{n}) < 0 \tag{29a}$$

$$\hat{h} = \tfrac{1}{2}\hat{T}_w\hat{g}, \quad \text{for} \quad (V\cdot\boldsymbol{n}) < 0 \tag{29b}$$

where $\boldsymbol{n}$ is the inward normal vector to the surface. The wall number flux $\hat{n}_w$ is not known a priori, and may be determined by applying the condition of no net flux normal to the surface:

$$\hat{n}_w = -2(\pi/\hat{T}_w)^{1/2}\int_0^\infty\int_\phi (V\cdot\boldsymbol{n})\hat{g}V\,\mathrm{d}V\,\mathrm{d}\phi, \quad \text{for} \quad (V\cdot\boldsymbol{n}) > 0 \tag{30}$$

Along the centerline, symmetric boundary conditions are used

$$\hat{g}(\xi, \eta = 0, \phi) = \hat{g}(\xi, \eta = 0, \pi - \phi) \tag{31a}$$

$$\hat{h}(\xi, \eta = 0, \phi) = \hat{h}(\xi, \eta = 0, \pi - \phi) \tag{31b}$$

### Numerical Procedure

In each iteration step, the calculation starts at the point ($\eta = 2 - \Delta\eta$, $\xi = -2 + \Delta\xi$) for a chosen discrete ordinate $V_\delta$. For this discrete ordinate, the values of the distribution functions are then determined at all ($\xi$, $\eta$) grid points for the quadrant of velocity angle $\pi/2 \le \phi \le \pi$. Then, applying the symmetric conditions (31), the values of the distribution functions at the centerline are determined for the quadrant of velocity angle $\pi/2 \ge \phi \ge 0$, and calculated at all ($\xi$, $\eta$) grid points starting from the point ($\eta = \Delta\eta$, $\xi = -2 + \Delta\xi$). An analogous procedure is carried out for the quadrant of velocity angle $-\pi \le \phi \le -\pi/2$, and $-\pi/2 \le \phi \le 0$ starting from the point ($\eta = 2 - \Delta\eta$, $\xi = 2 - \Delta\xi$) and ($\eta = \Delta\eta$, $\xi = 2 - \Delta\xi$), respectively. After this procedure is repeated for all discrete ordinates $V_\delta$ for both $\hat{g}_\delta$ and $\hat{h}_\delta$, the wall number flux $\hat{n}_w$ and the moments may be calculated by means of the quadrature formula [Eq. (12)], with a proper integration method over the angle. The iterative procedure is stopped when the differences of all moments between two iterative steps $I + 1$ and $I$, $|(M^{I+1} - M^I)/M^I|$, are less then $10^{-3}$ for all spatial grid points. In the following, some of the results calculated by means of the above described method are reported. As a proper quadrature formula, the modified Gauss-Hermite half range quadrature for integrals of the form[15]

$$\int_0^\infty \exp(-y^2) y^w Q(y)\, dy \tag{32}$$

is used for $w = 1$ with 8th-order discrete ordinate, and Simpson's $\frac{3}{8}$ rule with $\Delta\phi = 4.5$ deg is used for the integration over the angle $\phi$. The ($\eta$, $\xi$) plane was covered by $51 \times 21$ grid points for the upstream reservoir, $31 \times 81$ for the channels, and $51 \times 31$ for the downstream reservoir. An increase in the number of grid points in the $\eta$ and $\xi$ directions showed a negligible change in the solution values. The values of the stretching parameters were chosen to be $t_x = t_y = 0.3$ and $t_n = 1.9$. The constant of the viscosity-temperature relation in Eq. (25) $\sigma$ was that for Argon, 0.811. The surface temperature and the temperature in the far downstream reservoir were chosen to be the same as that in the far upstream reservoir.

## Results

### Free-Molecular Flow

For the case of free-molecular flow, there are no collisions between molecules, and molecules are moving without collision until reaching the surface of a body. Thus, at any point in the physical space, the velocity space can be divided into two regions, one for molecules coming from the reservoirs and the other for molecules emitted from the surface. Since exact values of the distribution function can be obtained for each region, theoretical values of moments for free-molecular flow conditions may be obtained by numerically integrating the distribution function.[9] The free-molecular solution may serve as a good standard for checking the accuracy of a finite difference approximation.

Figure 2 shows the free-molecular wall number flux for convergent or divergent slots for a hard vacuum in the downstream reservoir. The symbols show Reynolds and Richley's[9] theoretical wall number flux obtained by numerical integration of distribution functions, and the solid lines show the results of the present finite difference approximations for the case of a length to width ratio $L/W = 1.0$. The differences between the finite difference approximations and Reynolds and Richley's results were less than 2.0% for the cases of wall half-angle less than 30 deg. In Fig. 3, the free-molecular centerline fluxes for convergent or divergent slots are compared. The solid lines show the results of the finite difference approximations, and the symbols show those of Reynolds and Richley.[9]

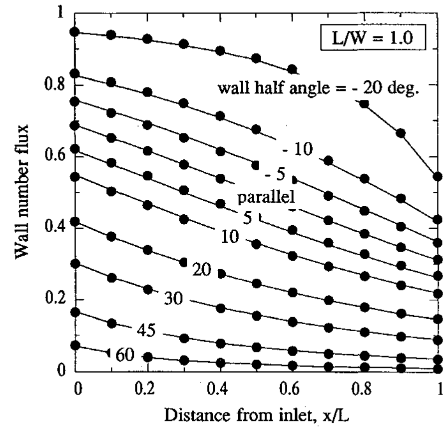


**Fig. 2 Comparison of free-molecular wall number flux.**

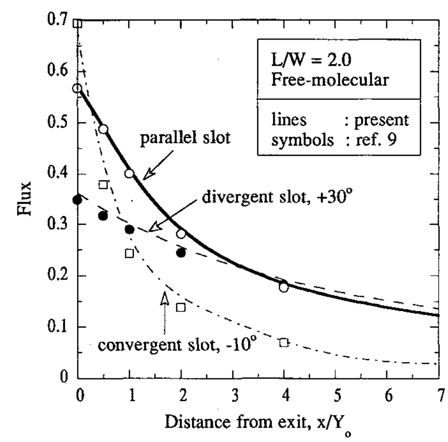


**Fig. 3 Free-molecular flux along centerline.**

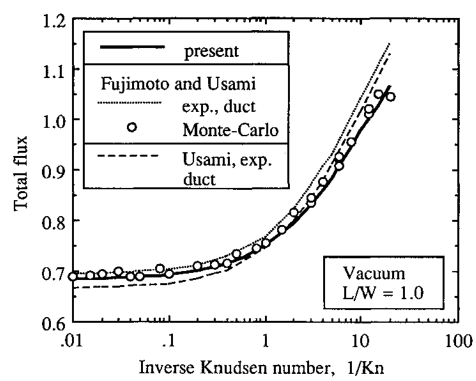


**Fig. 4 Comparison of total flux through parallel slot.**

### Parallel Slot

For flow through a parallel slot, the total flux at arbitrary Knudsen number for the case of $L/W = 1.0$ and hard vacuum in the downstream reservoir is compared with the Monte Carlo simulation and experimental results of Fujimoto and Usami,[7] and the experimental results of Usami.[34] The solid line in Fig. 4 shows the result of the finite difference approximation, the circles the Monte Carlo simulation result,[7] and the dotted line the experimental result of Fujimoto and Usami[7] for the case of a rectangular duct that has the ratio of long side to short side of 26.63 and $L/W = 0.995$. The dashed line is the experimental result of Usami[34] for the case of a rectangular duct that has the ratio of long side to short side of 28.27 and $L/W = 1.008$. Our results agree very well with the Monte Carlo simulation results.

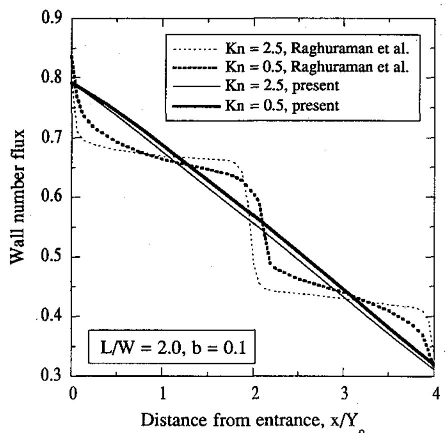


**Fig. 5 Wall number flux distribution.**

Figure 5 shows the predicted wall number flux in a parallel slot of $L/W = 2.0$ with a finite downstream pressure ratio of 0.1 at Knudsen numbers 2.5 and 0.5. The solid lines show the results of the finite difference approximations, and the dotted lines show those of Raghuraman and Willis,[5] who solved the Boltzmann equation with the BGK model by the moment and discrete ordinate methods and obtained a mass flux and a wall number flux. Their results follow the overall trend of the finite difference approximations, but have step-like variations, which is incorrect in a physical sense. This is attributable to the fact that in their solution the only oblique angular direction considered in the velocity space was $\pi/4$ with respect to the slot axis, as was pointed out in their paper. Also, Raghuraman and Willis[5] neglected the variation of flow in the reservoirs and assumed Maxwell distributions characterized the reservoir conditions, which is incorrect except for the case of free-molecular flow.

### Nozzle with Arbitrary Contour

The geometry of a sample nozzle used in the present investigation is shown in Fig. 6. The Mach contours around the sample nozzle for hard vacuum or finite pressure downstream reservoir conditions are shown in Figs. 7 and 8, respectively, for $Kn = 5.0$ and 0.05. The Mach number is based on the speed of sound at the upstream reservoir condition. The decrease of the Knudsen number, i.e., the increase of the intermolecular collisions, increases the flux through the nozzle and, thus, the Mach number in the overall flowfield. For the case of hard vacuum downstream pressure, the flow continuously accelerates and gradually approaches a certain limit in the plume region. This is due to the fact that, in the case of a considerably low downstream pressure, the contribution of each molecule to the macroscopic velocity increases as $x$ increases, because the number of molecules moving in the negative $x$ direction decreases and only the molecules that have a relatively pure positive $x$ component remain in the domain of integration. A slight increase in the downstream reservoir pressure increases the number of molecules with a negative $V_x$ component. They affect the flow velocity $U_x$ and retard it in the plume region. Any further increase in the downstream reservoir pressure will severely alter the velocity profile inside the nozzle, as can be seen in Fig. 8. Thus, the variation of macroscopic velocity in the plume region and inside a nozzle will depend on the pressure ratio, nozzle geometry, and Knudsen number. This kind of flow situation may be found in freejet experiments.[35,36] In the case of continuum flow, a barrel shock and Mach disc may appear instead of smooth changes in the macroscopic variables.[36]

Figure 9 shows the effect of the downstream reservoir pressure on the Mach number along the centerline for the sample nozzle in the case of a free-molecular flow. It can be seen that the flow can have a maximum Mach number either inside

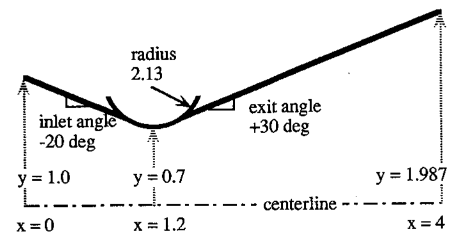


**Fig. 6 Geometry of sample nozzle.**

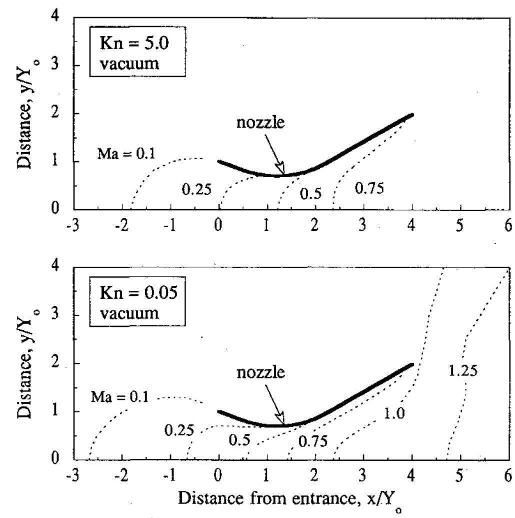


**Fig. 7 Mach contours for the case of hard vacuum.**

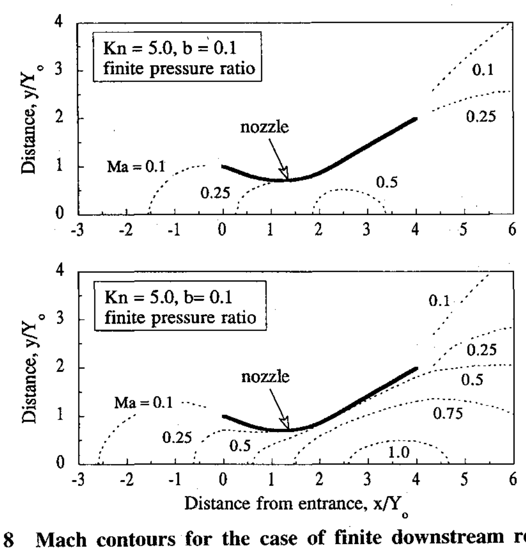


**Fig. 8 Mach contours for the case of finite downstream reservoir pressure.**

the nozzle or in the plume region, depending on the induced downstream pressure.

The variations of exit plane velocity distribution at Knudsen number 0.05 for various channel geometries are shown in Fig. 10. A convergent channel has a flatter exit velocity profile than a parallel or a divergent channel. The chance that the molecules that do not have a relatively pure positive $V_x$ component will collide with the channel surface is higher in the case of convergent channels than in the case of parallel or divergent channels. The surface that is facing the upstream direction increases the chance of colliding molecules to be backscattered. Thus, the decrease in the exit-to-entrance area ratio causes the exit plane flow velocity profile to be flatter. The slip condition is noticed at the nozzle wall, and a divergent channel shows more velocity slip than a parallel or a conver-

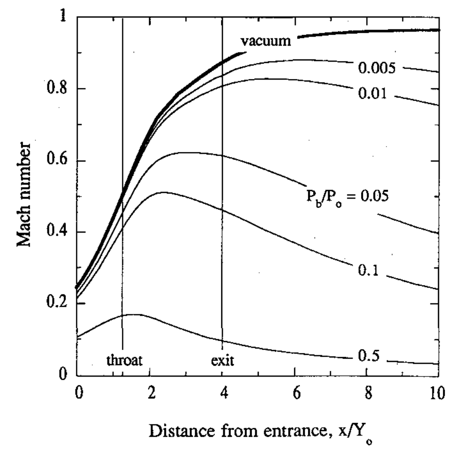


**Fig. 9 Mach number variation with downstream pressure along the centerline for the sample nozzle (free-molecular flow case).**

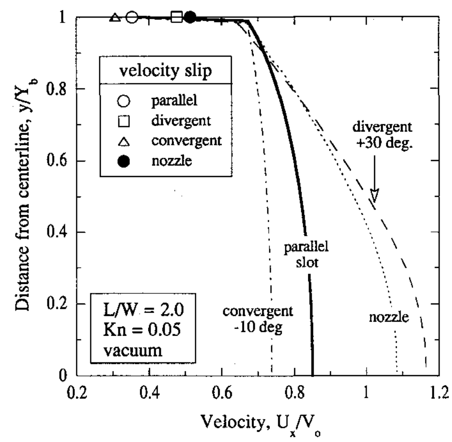


**Fig. 10 Velocity distribution at exit plane.**

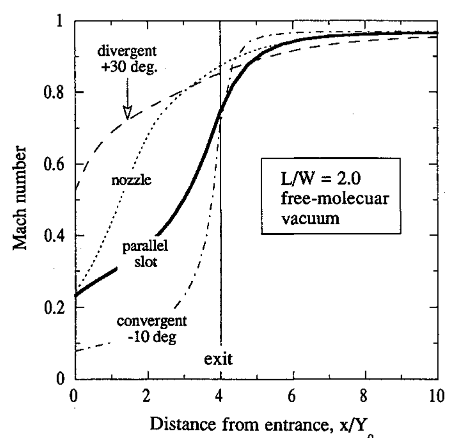


**Fig. 11 Mach number variation along centerline due to channel geometry.**

gent one. This is due to the fact that as the exit-to-entrance area ratio increases, the density decreases and the local Knudsen number increases, and thus the flow becomes more rarefied at the exit plane.

The variations of centerline Mach number for free-molecular flow for various channel geometries are shown in Fig. 11. A convergent channel experiences a more abrupt change in the Mach number at the exit plane due to the free expansion of a higher density flow than in the cases of a parallel or a divergent channel.

## Conclusions

A kinetic theory analysis has been made to describe the flow of rarefied gases through two-dimensional nozzles with arbitrary contour. The present investigation is based on the solution of a set of simplified Boltzmann equations, in which the collision integral was replaced by a model equation. The general grid-generation technique and the finite difference approximation with the discrete ordinate method have been shown to be a practical method for treating the flow of rarefied gases through complex geometries in the transition regime. To demonstrate the feasibility of the method, calculations were made for the flow through parallel, convergent, and divergent slots. Results for free-molecular flow compared very well with those calculated from theoretical distribution functions. Comparison of the predicted total flux through parallel slots showed good agreement with the existing literature data. New results for the case of convergent or divergent slots, and for a nozzle with arbitrary contour at arbitrary Knudsen number for both hard vacuum and finite downstream pressure conditions have been presented.

## Acknowledgments

This work was sponsored in part by the NASA Lewis Research Center, Cleveland, Ohio, under Grant NAG 3-577. Earl Morren is the Grant Director.

## References

[1] Willis, D. R., "Mass Flow Through a Circular Orifice and a Two-Dimensional Slit at High Knudsen Numbers," *Journal of Fluid Mechanics*, Vol. 21, No. 1, 1965, pp. 21–31.

[2] Wang, P. Y., and Yu, E. Y., "Nearly Free-Molecular Slit Flow at Finite Pressure and Temperature Ratios," *Journal of Fluid Mechanics*, Vol. 50, No. 3, 1971, pp. 565–577.

[3] Liepmann, H. W., "Gaskinetics and Gasdynamics of Orifice Flow," *Journal of Fluid Mechanics*, Vol. 10, No. 1, 1961, pp. 65–79.

[4] Wang, P. Y., and Yu, E. Y., "Nearly Free-Molecular Channel Flow at Finite Pressure Ratio," *Physics of Fluids*, Vol. 15, No. 6, 1972, pp. 1004–1009.

[5] Raghuraman, P., and Willis, D. R., "Kinetic Theory Analysis of Rarefied Gas Flow Through Finite Length Slots," *Physics of Fluids*, Vol. 20, 1977, pp. 895–902.

[6] Yamamoto, K., and Asai, M., "Nearly Free Molecular Flow Through a Two-Dimensional Channel of Finite Length," *Rarefied Gas Dynamics*, edited by R. Campargue, Commissariat a l'Energie Atomique, Paris, 1979, pp. 219–228.

[7] Fujimoto, T., and Usami, M., "Monte-Carlo Simulation on Rarefied Gas Flow Through Two-Dimensional Slits (Cases of High Pressure Ratio)," *Nippon Kikai Gakkai Ronbunshu*, B-hen, Vol. 50, No. 459, 1984, pp. 2717–2722.

[8] Usami, M., Fujimoto, T., and Kato, S., "Monte-Carlo Simulation on Mass-Flow Reduction Due to Roughness of a Slit Surface," *Rarefied Gas Dynamics*, edited by E. P. Muntz, D. P. Weaver, and D. H. Campbell, Vol. 116, Progress in Astronautics and Aeronautics, AIAA, Washington, DC, 1989, pp. 283–297.

[9] Reynolds, T. W., and Richley, E. A., "Free-Molecule Flow and Surface Diffusion Through Slots and Tubes—A Summary," NASA TR R-255, Nov. 1967.

[10] Füstöss, L., "Monte-Carlo Calculations for Free Molecular and Near-Free Molecular Flow Through Cylindrical and Conical Tubes," *Proceedings of the 7th International Vacuum Congress and 3rd International Conference on Solid Surfaces*, R. Dobrozemsky, Vienna, Austria, 1977, pp. 101–104.

[11] Bhatnagar, P. L., Gross, E. P., and Krook, M., "A Model for Collision Processes in Gases. I. Small Amplitude Processes in Charged and Neutral One-Component Systems," *Physical Review*, Vol. 94, No. 3, 1954, pp. 511–525.

[12] Bird, G. A., *Molecular Gas Dynamics*, Oxford Univ. Press, London, 1976.

[13] Riley, B. R., and Scheller, K. W., "Kinetic Theory Model for the Flow of a Simple Gas from a Two-Dimensional Nozzle," *Rarefied Gas Dynamics*, edited by E. P. Muntz, D. P. Weaver, and D. H. Campbell, Vol. 116, Progress in Astronautics and Aeronautics, AIAA, Washington, DC, 1989, pp. 352–362.

[14] Huang, A. B., and Giddens, D. P., "A New Table for a Modified (Half-Range) Gauss-Hermite Quadrature with an Evaluation of the

Integral," *Journal of Mathematics and Physics*, Vol. 47, 1968, pp. 213–218.

[15]Shizgal, B., "A Gaussian Quadrature Procedure for Use in the Solution of the Boltzmann Equation and Related Problems," *Journal of Computational Physics*, Vol. 41, No. 2, 1981, pp. 309–328.

[16]Holway, L. H., Jr., "New Statistical Model for Kinetic Theory: Method of Construction," *Physics of Fluids*, Vol. 9, No. 9, 1966, pp. 1658–1673.

[17]Shakhov, E. M., "Generalization of the Krook Kinetic Relaxation Equation," *Fluid Dynamics*, Vol. 3, No. 3, 1968, pp. 95, 96.

[18]Abe, T., and Oguchi, H., "A Hierarchy Kinetic Model and Its Applications," *Rarefied Gas Dynamics*, edited by J. L. Potter, Vol. 51, Progress in Astronautics and Aeronautics, AIAA, New York, 1977, pp. 787–793.

[19]Morse, T. F., "Kinetic Model of Gases with Internal Degrees of Freedom," *Physics of Fluids*, Vol. 7, No. 2, 1964, pp. 159–169.

[20]Rykov, V. A., "A Model Kinetic Equation for a Gas with Rotational Degrees of Freedom," *Fluid Dynamics*, Vol. 10, No. 6, 1975, pp. 959–966.

[21]Sirovich, L., "Kinetic Modeling of Gas Mixtures," *Physics of Fluids*, Vol. 5, No. 8, 1962, pp. 908–918.

[22]Hamel, B. B., "Kinetic Model for Binary Gas Mixtures," *Physics of Fluids*, Vol. 8, No. 3, 1965, pp. 418–425.

[23]Garzó, V., Santos, A., and Brey, J. J., "Kinetic Model for Gases with Internal Degrees of Freedom," *Physics of Fluids A*, Vol. 1, No. 2, 1989, pp. 380–383.

[24]Chu, C. K., "Kinetic-Theoretic Description of the Formation of a Shock Wave," *Physics of Fluids*, Vol. 8, No. 1, 1965, pp. 12–22.

[25]Huang, A. B., "The Discrete Ordinate Method for the Linearized Boundary Value Problems in Kinetic Theory of Gases," Georgia Inst. of Technology, School of Aerospace Engineering, Rarefied Gas Dynamics and Plasma Lab. Rept. 4, Atlanta, GA, 1967.

[26]Chung, C. H., Jeng, D. R., De Witt, K. J., and Keith, T. G., Jr., "Flow of Rarefied Gases over Two-Dimensional Bodies," *Proceedings of the AIAA 9th Computational Fluid Dynamics Conference* (Buffalo, NY), 1989, pp. 389–399 (AIAA Paper 89-1970).

[27]Thompson, J. F., "Grid Generation Techniques in Computational Fluid Dynamics," *AIAA Journal*, Vol. 22, No. 11, 1984, pp. 1505–1523.

[28]Thompson, J. F., Warsi, Z. U. A., and Mastin, C. W., *Numerical Grid Generation: Foundations and Applications*, North-Holland, New York, 1985.

[29]Thomas, P. D., and Middlecoff, J. F., "Direct Control of the Grid Point Distribution in Meshes Generated by Elliptic Equations," *AIAA Journal*, Vol. 18, No. 6, 1980, pp. 652–656.

[30]Chung, C. H., Ph.D. Dissertation, Univ. of Toledo, Toledo, OH, 1990.

[31]Anderson, D. A., Tannehill, J. C., and Pletcher, R. H., *Computational Fluid Mechanics and Heat Transfer*, McGraw-Hill, New York, 1984.

[32]Roache, P. J., *Computational Fluid Dynamics*, Albuquerque, NM, 1982.

[33]Chapman, S., and Cowling, T. G., *The Mathematical Theory of Non-Uniform Gases*, Cambridge Univ. Press, London, 1958.

[34]Usami, M., private communication, Mie Univ., Kamihama-Cho, Tsu-Shi, Japan.

[35]Miller, D. R., Fineman, M. A., and Murph, H., "The Free Jet Expansion from a Capillary Source," *Rarefied Gas Dynamics*, edited by O. M. Belotserkovskii, M. N. Kogan, S. S. Kutateladze, and A. K. Rebrov, Plenum Press, New York, 1982, pp. 923–930.

[36]Fujimoto, T., Kato, S., Usami, M., Niimi, T., and Kamiya, S., "A Study on the Structure of Free-Jets of Mixture by Laser-Induced Fluorescence," *Rarefied Gas Dynamics*, edited by H. Oguchi, Univ. of Tokyo Press, Tokyo, 1984, pp. 467–475.